

2000

DHA

Fourth Annual Report

on the

Mechanical Behavior of Polycrystalline Ceramics

Brittle Fracture of SiC - Si₃N₄ Materials

(NASA-CR-136704) MECHANICAL BEHAVIOR OF
POLYCRYSTALLINE CERAMICS: BRITTLE FRACTURE
OF SiC - Si₃N₄ MATERIALS Annual
Report (Kentucky Univ.) 45 p HC

N74-16245

CSCL 11D 63/18 Unclas
15711

submitted to

The Lewis Research Center of

The National Aeronautics and Space Administration

Cleveland, Ohio

as part of

NASA Grant NGL 18-001-042

September 1, 1973

Submitted by:

Martin H. Leipold
Associate Professor of
Materials Science

Cawas M. Kapadia
Research Assistant

Anant H. Kelkar
Research Assistant

Kentucky Univ.
Lexington

Reproduced by
NATIONAL TECHNICAL
INFORMATION SERVICE
US Department of Commerce
Springfield, VA. 22151



N O T I C E

**THIS DOCUMENT HAS BEEN REPRODUCED FROM
THE BEST COPY FURNISHED US BY THE SPONSORING
AGENCY. ALTHOUGH IT IS RECOGNIZED THAT CER-
TAIN PORTIONS ARE ILLEGIBLE, IT IS BEING RE-
LEASED IN THE INTEREST OF MAKING AVAILABLE
AS MUCH INFORMATION AS POSSIBLE.**

INTRODUCTION

This report describes the results of the final stages of the research involving the role of anions in the behavior of magnesium oxide, as well as the continued efforts of the fracture behavior of silicon nitride materials. These efforts, particularly the first, are further sub-divided in subsections describing individual types of behavior of materials.

Part I. Oxide Research

This research was designed to define the importance of typical anion impurities such as sulphur, chlorine, fluorine, and hydroxyl in the behavior of a typical ceramic such as magnesium oxide. All experimental phases of research at this laboratory has been completed and majority of the results have been reported in the open literature. In several cases additional reports are still in progress and will be completed shortly.

Section I. Fabrication

The results of the fabrication studies appeared in the Journal of the American Ceramics Society, Vol. 56, No. 4, April 1973 in a paper entitled "Affect of Anions on Hot-Pressing of MgO" by M. H. Leipold and C. M. Kapadia.

Section II. Grain Boundary Micro-hardness

The experimental results here have been completed and some additional analysis conducted. At the present time the results do not appear to indicate significant differences among the behavior of the various dopants. At present it is not clear if these negative results are themselves significant, that is indicating a lack of an effect, or whether the experimental techniques was not sufficiently sensitive. Some additional attempts to resolve this question may be made. No additional experiments will be conducted.

Section III. Grain Growth

The experimental work on the effect of anions on grain growth in MgO has been completed. A number of papers have been published or accepted for publication as a result of this phase of the work. The first appeared in the Journal of the American Ceramic Society, Vol. 56, No. 5, May 1973, entitled "Interrelation of Pore Size and Grain Size During Grain Growth of Oxide" by C. M. Kapadia and M. H. Leipold.

A second paper entitled, " O^{2-} Mobility in Grain Growth in Pure Dense MgO" has been submitted to the American Ceramic Society. A third paper, "A Review of the Mechanism of Grain Growth in Polycrystalline Ceramics" has also been submitted to the American Ceramic Society. A fourth paper, entitled, "Grain Boundary Mobility in Anion Doped MgO" has been submitted and accepted by the Symposium on Surfaces and Interfaces of Glass and Ceramics, to be held at Alfred University, Alfred, N. Y. August 27-29, 1973. In addition, a doctoral dissertation by C. M. Kapadia will be completed.

Section IV. Diffusion

Previous reported results indicated that $1200^{\circ}C$ anion impurities had no affect on the grain boundary mobility of Ni^{+2} in magnesium oxide. It had been anticipated that an affect might be noted since the anions could be expected to affect the defect structure in the MgO. These results were reported at the 74th Annual Meeting of the American Ceramics Society at Washington in 1972. Additional diffusion anneals have been prepared covering in the range of 1000 to $1400^{\circ}C$ to determine any affect on the activation energy for diffusion. The samples have been sent to H. Stadelmaier at North Carolina State University for analysis. Results have not as yet been obtained and when they are, they will be written up for publication.

Section V. Mechanical Analysis

No additional research has been conducted in this area.

Part II. Silicon Nitride-Silicon Carbide Research

Introduction

A characteristic of rupture of some ceramics like silicate glass and oxides is that the measured strength depends on the length of time a load is applied or on the loading rate. Although these materials can withstand quite high stresses for a short period of time, low stress will ultimately lead to fracture if applied for a sufficiently long period of time. This is static fatigue. A slow crack growth occurs till the crack length reaches a critical value at which catastrophic fracture occurs. The time during which the crack grows slowly at a particular stress level before a critical condition is reached can give us an idea about the time period for which a machine component would last at that stress level or the life of the component.

Silicon nitride and silicon carbide are very useful structural materials for high temperature application such as in gas-turbine engines because of their high fracture energy, low coefficient of thermal expansion, good thermal conductivity, inherent corrosion and abrasion resistance to gaseous environment and high temperature stability. The purpose of the present work was to see whether slow crack growth occurred in these materials at room temperature. A modified method of fracture toughness testing which applies a constant moment to a specimen was used in this work to control and measure crack velocity. Glass, plexiglass, H. P. Si_3N_4 (HS-130 Norton), SiC (REFEL), SiC (Ceradyne) were tested using this technique.

Testing the Performance of the Jig

The principle of the technique used here and the design of the jig to apply this technique has already been reported.¹ The performance on the jig was first evaluated to see the suitability of this jig for the modified fracture toughness testing.

The crack velocity is measured in terms of the deflection of arm I (See Fig. 1) of the jig as the crack propagates, it is essential to know any component of the deflection of the arm I due to elastic deformation of the jig itself.

A hardened tool steel CMB specimen was prepared and the load-deflection behavior of the jig was studied with this specimen. A maximum load of 50 kg in the arm II of the jig is calculated to fracture HP Si₃N₄ specimen. Therefore, the jig was tested to a load of 100 kg in Instron with the tool steel specimen for a factor of safety equal to 2. This corresponds to a load of 200kg indicated by the Instron. The deflection in the arm I of the jig was recorded by a transducer. For 200 kg. load, a deflection of 0.025 inch was observed.

To locate the source of this deflection, the theoretical deflection of the arm I of this jig due to the elastic deformation of the specimen arm was calculated.

Theoretical Deflection

In Fig. 2, moment acting on the arm of this specimen

$$= M = 100 \text{ kg} \times 2.5 \text{ cm} = 250 \text{ kg-cm.}$$

Assuming the system to be cantilever beam,

Equation of the moment is

$$EI \frac{d^2 y}{dx^2} = M$$

where E = elastic modulus of this material of the specimen

$$= 2.11 \times 10^6 \text{ kg/cm}^2$$

I = moment of inertia of the cross section area of the specimen arm about the neutral axis

$$= 0.0102 \text{ cm}^4$$

Integrating this equation,

$$\therefore EI \frac{dy}{dx} = Mx + C$$

$$\text{At } x = 0, \frac{dy}{dx} = 0$$

$$\therefore C = 0$$

$$\therefore \tan \theta = \frac{dy}{dx} = \frac{Mx}{EI}$$

$$\therefore \tan \theta = (\text{at } x = 0.45 \text{ cm}) = 5.2 \times 10^{-3}$$

\therefore The theoretical deflection of the arm I of the specimen at point P = $y' = 0.0295$ inch.

The theoretical and experimental values of the deflection agree fairly well, indicating that the deflection observed must be due to the elastic deformation of the specimen.

To know the component of the deflection only due to the elastic deformation of the jig, two 1/4" thick steel plates were fastened tightly to the arms of the jig (Fig. 3) and the load up to 200 kg was applied with the Instron. The deflection-load plot for loading and unloading is shown in Fig. 4 . The plot shows linear relationship between load and deflection which is as expected. Deflection of 0.006 inch was observed for a load of 200 kg. The loading and unloading curves include a very small area. This indicates that the jig comes back to its original configuration after the load is removed, i. e., there is no plastic deformation of the jig up to load of 200 kg.

The above experiments indicate that the jig should work for the fracture toughness testing with CMB specimen of HP Si₃ N₄ . The component of the deflection due to elastic deformation of the jig, which is to be subtracted from the actual deflection observed at a particular load is also obtained.

Specimen Configuration and Formulae to be Used

The geometry of the specimen used for this testing was different from the Double Cantilever Beam specimen configuration used in conventional fracture toughness testing. This geometry was chosen so that a rigid 3-line grip could be used to transmit the moment from the jig to the specimen. (See Figs. 1&5). The formulae used for calculation of fracture toughness using DCB specimen had to be modified here to take care of the change in geometry of the specimen.

For the DCB specimen, the formula for fracture toughness is

$$G_c = \frac{12F^2 L^2}{EWb^3} \left[\underset{\text{1st term}}{1} + \underset{\text{2nd term}}{1.32 \left(\frac{t}{L} \right)} + \underset{\text{3rd term}}{0.542 \left(\frac{t}{L} \right)^2} \right]$$

E = Elastic modulus of the material

F = Load of fracture

Other terms defined in Fig. 6a.

The first term is due to the bending moment energy supplied to the specimen when load F is applied to it. The third term is the shear energy term and the second term accounts for deformation beyond the crack tip.

We will consider modification to the three terms separately. With the first, the bending moment energy stored in a length ℓ and due to a bending moment m , producing a deflection on θ in the specimen arm is given by

$$\begin{aligned}
 U_{\text{bending}} &= \int_0^{\ell} \frac{1}{2} m \theta \, dx \\
 &= \int_0^{\ell} \frac{m^2}{2EI} \, dx \quad \text{where } I = \text{moment of inertia of the cross section.} \\
 &= \int_0^{\ell} \frac{F^2 x^2}{2EI} \, dx \quad \text{where } m = Fx \\
 &= \frac{F^2 \ell^3}{6EI}
 \end{aligned}$$

The rate of change of bending moment energy stored in one surface of the specimen = $\frac{du_{\text{bending}}}{dx}$

$$\begin{aligned}
 &= \frac{F^2 \ell^2}{2EI} \\
 &= \frac{6F^2 \ell^2}{Ewt^3}
 \end{aligned}$$

Since fracture of the specimen produces two surface, the total rate of change of bending moment energy

$$= \frac{12 F^2 \ell^2}{Ewt^3}$$

Since in this specimen the shaded portion is missing (Fig. 7), the total rate of change of bending moment energy will be

$$\begin{aligned}
 &= \frac{12 F^2 \ell^2}{Ewt^{*3}} + \frac{12 F^2 (L - \ell)}{Ewt^3} \\
 &= \frac{12 F^2 L^2}{Ewt^3} + \frac{12 F^2 \ell^2}{Ew} \left(\frac{1}{t^{*3}} - \frac{1}{t^3} \right) \\
 &= \frac{12 F^2 L^2}{Ewt^3} \left\{ 1 + \frac{\ell^2}{L^2} \left[\left(\frac{1}{t^{*3}} - 1 \right) \right] \right\}
 \end{aligned}$$

Similiarly, the modification for the second term will be

$$1.32 \left(\frac{t}{L} \right) \left\{ 1 + \left(\frac{\ell}{L} \right) \left[\left(\frac{t}{t^*} \right)^2 - 1 \right] \right\}$$

and third term will be

$$0.542 \left(\frac{t}{L} \right)^2 \left\{ 1 + \left(\frac{\ell}{L} \right)^2 \left[\left(\frac{t}{t^*} \right)^2 - 1 \right] \right\}$$

Therefore, the formula for fracture toughness using this modified specimen and conventional fracture toughness testing (DCB) will be

$$\begin{aligned} G_c = & \frac{12F^2 L^3}{Ewbt^3} \left\{ 1 + \left(\frac{\ell}{L} \right)^2 \left[\left(\frac{t}{t^*} \right)^3 - 1 \right] \right. \\ & + 1.32 \left(\frac{t}{L} \right) \left\{ 1 + \left(\frac{\ell}{L} \right) \left[\left(\frac{t}{t^*} \right)^2 - 1 \right] \right\} \\ & \left. + 0.542 \left(\frac{t}{L} \right)^2 \left\{ 1 + \left(\frac{\ell}{L} \right)^2 \left[\left(\frac{t}{t^*} \right)^2 - 1 \right] \right\} \right\} \quad (\text{Eqn I}) \end{aligned}$$

For fracture toughness testing with constant moment (CMB) geometry specimen, the fracture toughness is given by

$$G_c = \frac{12 M^2}{Ewbt^3}$$

where M = moment applied

Similarly taking care of the shaded removed portion in CMB specimen (Fig. 6b) the fracture toughness will be given by

$$G_c = \frac{M^2}{Ewbt^3} \left\{ 1 + \left(\frac{\ell}{L_c} \right)^2 \left[\left(\frac{t}{t^*} \right)^3 - 1 \right] \right\} \quad (\text{Eqn II})$$

$$\begin{aligned} \text{The crack velocity } \frac{da}{dT} \\ = \frac{EI}{ML_t} \frac{d\delta}{dT} \end{aligned}$$

where

$$\frac{d\delta}{dT} = \text{rate of change of deflection of tip of the transducer.}$$

I = moment of inertia of the cross section of the

L_t = distance of the transducer from the fulcrum

M = the moment applied to each arm of the specimen and equals $(\frac{p_1 + p_3}{2}) L_c + p_2 L_t$ and p_1 is the measured fracture load

p_2 is the weight of the micrometer or its counterbalance. (. 1 kg).

p_3 is the weight of the lower jig arm (cross hatched in Fig. 1) + arms II. = 1.05 kg.

L_t is the arm length to the transducer.

L_c is the lever arm length

Experimental Procedure

Preparation of fracture specimens out of HP Si_3N_4 HS-130 is extremely time consuming. To simplify the specimen preparation, easily available materials like glass and plexi-glass were used to establish all the experimental details and the specimen geometry.

These materials were available in sheet form and were easily cut and machined to the desired shape by conventional (plexiglas) or routine diamond (glass) techniques. The configuration is in Figure 7.

The procedure which was finally developed (See Fig. 8) for the Si_3N_4 (suitable for carbides as well) is as follows:

1. Slabs ($1\frac{1}{2}$ " x $1\frac{1}{2}$ " x .1") were cut on a precision wafering machine using an available diamond wheel.* Very slow rates were required (.025 depth/pass at 0.125 in/min pass speed) and the wheel required redressing after each pass. A different wheel[†] was superior (.05 depth/pass at 0.4 in/min) but redressing still required.
2. A diamond core drill (3/8 in. diam.) was used (Fig. 8, Step b) and it was necessary to drill part way through from side, turn the piece over, and finish from the other side to avoid chipping the second surface. A 1/4" core drill was used to smooth the hole interior. The material between the arms was cut with the diamond saw (Fig. 8, Step C).
3. A groove halfway deep (Fig. 8, Step d) was cut.
4. A notch was made in the specimen with diamond drill (Fig. 8, Step e). The length of the notch was found to be

* Norton 5 x 0.019 x 0.625 D220-N100M-1/8

† Norton 6 x 0.025 x 0.625 SD150-R100B69-1/8

critical in ease of producing microcrack and length of 3-5 mm was found to be ideal.

5. The last step in making the specimen was to produce a microcrack (Fig. 8, Step f). In either fracture toughness test (CMB or DCB), the specimen is fractured by the extension of a microcrack produced in the specimen. The specimen without any crack was held (lightly tightened) in the middle at 3 to 4 mm from the tip of the notch with a hardened tool steel clamp and the load was applied with tensile testing machine[†] at a crosshead speed of 0.0002 in/min. At a particular load a crack was produced at the tip of the notch along the side groove and propagated until it was arrested by the compressive stress field produced by the clamp on the specimen. The crack propagation is indicated by a sudden small drop in the load and exactly at that instant, the crosshead motion is reversed to reduce the load. The distance at which the clamp was tightened from the tip of the notch, the amount of tightening and the cross head speed during application of load were found to be critical in producing the microcrack and the suitable values were found by trial error.

After cracking, all specimen dimensions were recorded and the crack length L was measured with a microscope.

Conventional fracture toughness testing using the modified CMB specimen form was accomplished by using only parts I (the three line grip) and part II of the CMB jig. See Fig. 1. The specimen containing the microcrack was held with the grip of part I by tightening the screws.

[†]Instron

Parts II were connected to part I and to the testing machine thus lying parallel rather than perpendicular to part I. Load was applied to the specimen by downward crosshead motion of the tensile testing machine at crosshead speed of 0.002 in/min. The load at which the specimen fractured was noted.

The entire CMB assembly (Fig. 1) was used for the constant moment testing. The jig was attached to the instron and when it is hanging, the Instron was balanced to zero load and the transducer used to measure the the crack velocity was then calibrated. Loading was then started at desired crosshead speed. The microcrack in the specimen was constantly being observed with a telescope during loading. For glass and plexiglass specimens it was observed that when the crack started propagating in the specimen, the load almost remained constant till the specimen completely fractured. This constant load (P_1) was used to calculate the toughness value.

Crosshead speeds of 0.02, 0.002, 0.0002, 0.00002, cm/min, 0.05, 0.005, 0.00005 cm/min. were used (the very slow speeds were obtained by special gear reductions to the Instron). In all the cases, the fracture surfaces were carefully preserved.

Results for glass and plexiglass are shown in Tables I, II and III and Figs. 9 and 10.

With the initial tests of Si_3N_4 and SiC , the telescope was not used as a matter of convenience and the data for slow crack growth was taken solely from the transducer readings. These results had been reported previously and indicated the existence of slow crack growth in all of these materials. Question arose concerning these results and careful reanalysis of this data was made.

Since the data from which slow crack growth had been determined showed a slow but steady increase in load during the time in which the transducer indicated crack motion, analysis was made of the deflections in the specimen and jig. Prior to fracture in absence of slow crack growth, the

deflection δ_{el} indicated by the transducer consists of two parts.

$$\delta_{el} = \delta_s + \delta_j$$

where δ_s is due to the elastic deflection of the specimen arm due to the applied bending moment and δ_j is due to the elastic deformation of the jig itself.

$$\therefore \frac{d\delta}{dT} = \frac{d\delta_s}{dT} + \frac{d\delta_j}{dT}$$

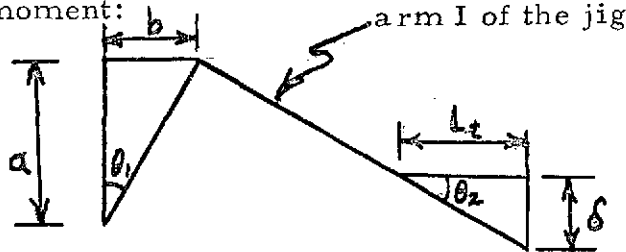
During the evaluation of the performance of the jig, δ_j vs load curve was plotted (Fig. 4). The slope of this curve gives $\frac{d\delta_j}{dF}$. From the load-time curve, $\frac{dF}{dT}$ is obtained and

$$\frac{d\delta_j}{dT} = \frac{d\delta_j}{dF} \times \frac{dF}{dT}$$

So $\frac{d\delta_j}{dT}$ can be obtained.

Also rate of change of moment $\frac{dM}{dT}$ applied on the specimen arm can be obtained and using the elastic theory of bending of beams, an estimate of $\frac{d\delta_s}{dT}$ is obtained.

Relationship between rate of change of deflection and rate of change of moment:



b = elastic deflection of the specimen

δ_s = deflection of the transducer due to elastic deformation of specimen arm

L_t = distance of the transducer from the fulcrum.

$$\theta_1 = \theta_2 \approx \tan \theta_2 = \frac{b}{a} \approx -\frac{\delta}{L_t}$$

$$\theta \approx -\frac{Mx}{EI}$$

$$\text{For } x = a, \quad \theta_1 = -\frac{Ma}{EI}$$

$$\therefore b = \frac{Ma^2}{EI}$$

Also

$$\delta_s = \frac{aL_t}{EI} M$$

$$\therefore \frac{d\delta_s}{dT} = \frac{aL_t}{EI} \frac{dM}{dT}$$

since a, L_t, I are constant prior to crack propagation.

For this configuration, we can then calculate

$$\frac{d\delta_{el}}{dt} = \frac{d\delta_s}{dt} + \frac{d\delta_j}{dt} =$$

$$\frac{aL_t}{EI} \frac{dM}{dT} + \frac{d\delta_j}{dF} \times \frac{dF}{dT}$$

and using measured values of $\frac{dM}{dT}$ for each data set, $\frac{d\delta_j}{dF}$ from initial jig evaluation (Fig. 4) and A, L_t, E, I from the specimen, it was determined that calculated elastic deflections and observed deflections agreed within a scatter of +10%. This was one confirmation of lack of slow crack growth.

To further evaluate the question of slow crack growth occurring in these materials, the specimen was subjected to a constant load for a long time.

Specifically, a modified specimen of SiC (REFEL) with dimensions $t = 1.15$ cm, $t^* = 0.7$ cm, $w = 0.067$ in, $b = 0.033$ in. was subjected to load 10.4 kg = p_1 using the modified method (CMB) with $l = 1.5$ cm $L_c = 3.81$ cm. This load corresponds to 80% of G_c average ($80,000$ ergs/cm²) for SiC(REFL). Initially, the load was applied with crosshead speed of 0.0002 cm/min. When the load reached 10.5 kg, the crosshead motion was stopped and the specimen was left loaded for one day. No decrease in load was observed during this time except in the first 2-3 minutes in which the load dropped to 10.4 kg due to slop in the testing machine. When reloading was started at crosshead speed 0.0002 cm/min., the specimen fractured suddenly at $p_1 = 11.2$ kg which gives value of fracture toughness G_c as

76190 ergs/cm². That is, the specimen was loaded for one day at load corresponding to 87.6% of the observed value of G_c . If slow crack growth had taken place in the specimen, the load would have slowly dropped as the crack proceeded. Since this did not occur, lack of slow crack growth is again indicated.

Consequently, all data for SiC and Si₃N₄ is presented as average values of G_c with standard deviation rather than as a function of velocity. Data for these refractories are given in Tables IV through IX.

Correlation of the microstructure in the materials tested with fracture data is being attempted. Scanning microscope results are shown in Fig. 11-22.

Additional fracture results are being obtained on AVCO Si₃N₄, Norton SiC and Carborundum KT SiC.

References

1. S. W. Freiman et al., "Crack Propagation in Ceramics," Progress Notes, Report of Naval Research Lab Progress, Feb. 1972, p. 36.
2. G. P. Marshall et al., "The Correlation of Fracture Data for PMMA," Journal of Materials Science 8 (1973) pp. 138-140.

Table I

Toughness Results for Glass by Conventional
(DCB) Technique and Modified Specimen

$$E = 81.0 \times 10^{10} \text{ dynes/cm}^2$$

$$w = 0.3048 \text{ cm}$$

$$b = 0.1524 \text{ cm}$$

$$t = 1.27 \text{ cm}$$

$$t^* = 0.75 \text{ cm}$$

Sp. No.	ℓ cm	L cm	F kg	$G_{C, \text{conv.}}$ ergs/cm ²
1	0.45	2.0	2.6	8947.28
2	0.40	2.05	2.5	9149.4
3	0.43	2.15	2.45	9391.2
4	0.39	2.15	2.40	8502.2
5	0.42	2.10	2.5	9503.3
6	0.39	2.05	2.55	9311.6

Table II

Toughness Results for Glass by CMB Technique
and Modified Specimen

Sp. No.	Crosshead speed in/min.	P_1 kg	$\frac{d\delta_{el}^*}{dT}$ in/min. $\times 10^4$	$\frac{d\delta}{dT}$ in/min.	G mod. ergs/cm ²	Crack vel in/sec.
1	0.0005	2.2		13.3×10^{-4}	7362.7	0.01848
2	0.0005	2.1	.39	13.05×10^{-4}	6961.6	0.01865
3	0.0005	2.15		13.21×10^{-4}	7160.6	0.01862
4	0.005	2.35	3.7	15.1×10^{-3}	7986.0	0.2015
5	0.005	2.35		14.95×10^{-3}	7986.0	0.19955
6	0.005	2.3		14.5×10^{-3}	7775.4	0.19615
7	0.05	2.6	36.	28.6×10^{-2}	9082.0	3.5798
8	0.05	2.5		27.2×10^{-2}	8636.0	3.4914
9	0.05	2.55		29.1×10^{-2}	8857.0	3.68828
10	0.05	Broke on side				
11	0.0002 cm/min.	2.05	.16	5.1×10^{-4}	6742.4	0.002783
12	0.00002 cm/min.	1.9	.02	6.2×10^{-5}	6221.64	0.00034

* $\frac{d\delta_{el}}{dT}$ = calculated $\frac{d\delta}{dT}$ assuming no crack propagation occurred
resulting from elastic deflection in arms - see text.

Table III

Toughness Results for Plexi-glass (PPMA) by CMB
Technique Using Modified Specimen

$$E = 2.77 \times 10^{10} \text{ dynes/cm}^2$$

$$w = 0.11 \text{ in} \quad b = 0.055 \text{ in} \quad t = 1.27 \text{ cm} \quad t^* = 0.75 \text{ cm}$$

$$l = 0.4 \text{ cm} \quad L_c = 3.81 \text{ cm} \quad L_m = 7.7 \text{ cm}$$

Sp. No.	Crosshead speed cm/min	P ₁ kg	d δ /dT* est in/min	d δ / dT in/min	Crack vel. mm/sec	G mod ergs/cm ²
1	0.2	3.4				475,112
2	0.2	3.5				491,974
3	0.2	3.5				491,974
4	0.2	3.35				468,421
5	0.2	3.6				512,281
6	0.02	3.2	~0.0168	0.082	0.238	427,421
7	0.02	3.25		0.088	0.231	446,049
8	0.02	3.2		0.081	0.220	427,421
9	0.02	3.15		0.0804	0.209	406,493
10	0.02	3.2		0.0813	0.225	406,049
11	0.005	2.8	~0.00361	0.0196	0.0252	36,4161
12	0.005	2.7		0.0226	0.0242	347,120
13	0.005	2.7		0.020	0.0242	347,120
14	0.005	2.9		0.0185	0.0231	381,661
15	0.005	2.85		0.0201	0.0283	372,872
16	0.002	2.6	~0.0017	0.0087	0.00510	330,464
17	0.002	2.55		0.0085	0.00633	322,290
18	0.002	2.6		0.0096	0.00558	330,464
19	0.002	2.4		0.0077	0.00596	314,217
20	0.002	2.5		0.0082	0.00672	298,380
21	0.0002	2.3	~0.00014	0.00065	0.00016	282,952
22	0.00002	2.1	~0.00001	0.000073	0.000023	253,326

* See previous

Material : H. P. Si₃N₄ (HS-130 Norton)

Test: CMB

Specimen configuration: Modified

$$E = 3.12 \times 10^{12} \text{ dynes/cm}^2$$

$$t = 1.27 \text{ cm}$$

$$t^* = 0.75 \text{ cm}$$

$$l = 1.0 \text{ cm}$$

$$L_c = 3.81 \text{ cm}$$

Sp. No.	w cm	b cm	Crosshead speed cm/min	P ₁ kg	G _c Mod
1	0.259	0.132	0.02	16.1	74358.6
2	0.104	0.104	0.002	14.1	83347.1
3	0.252	0.125	0.0002	14.8	69192.2
4	0.263	0.132	0.00002	15.13	66716.2
5	0.260	0.135	0.005	17.7	86119.3
6	0.262	0.131	0.0005	16.1	74251.3
7	0.242	0.120	0.0002	16.1	87431.3
8	0.164	0.082	0.00002	9.7	76046.2
9	0.281	0.145	0.0005	17.8	74996.7

Material: SiC (Ceradyne)

Method: CMB

Specimen configuration: Modified

Density = 3.04 g/cm^3 $E = 3.64 \times 10^{12} \text{ dynes/cm}^2$

$l = 1.5 \text{ cm}$ $L_c = 3.81 \text{ cm}$ $t = 1.15$ $t^* = 0.7 \text{ cm}$

Sp. No.	w in	b in	Crosshead speed cm/min	P ₁ kg	G. mod ergs/cm ²
1	0.154	0.077	0.002	21.0	75237.6
2	0.154	0.077	0.0002	21.8	80202.9
3	0.154	0.077	0.00002	21.9	80764.4

Material: SiC (REFEL)

Test: Conventional DCB

Specimen configuration: Modified

Density = 3.06 gm/cm^3 $E = 3.66 \times 10^{12} \text{ dynes/cm}^2$

$t = 1.15 \text{ cm}$ $t^* = 0.7 \text{ cm}$

Sp. No.	w in	b in	ℓ cm	L cm	F kg	G_c Conv. ergs/cm ²
1	0.12	0.06	0.74	1.26	16.2	76151.9
2	0.115	0.057	0.82	1.31	15.6	80384.2
3	0.12	0.062	0.76	1.29	16.6	81228.5

Test: CMB

$t = 1.15 \text{ cm}$; $t^* = 0.7 \text{ cm}$ $L_c = 3.81 \text{ cm}$ $\ell = 1.5 \text{ cm}$

Sp. No.	w in	b in	Crosshead speed cm/min	P_1 kg	G mod. ergs/cm ²
1	0.11	0.055	0.00002	15.2	81113.3
2	0.12	0.006	0.0002	16.3	77365.8
3	0.084	0.042	0.0002	11.5	82875.4
4	0.105	0.053	0.009	14.4	79491.5
5	0.12	0.062	0.00002	17.0	83518.0

Material: H. P. Si_3N_4 (HS-130 Norton)

Test: CMB

Specimen: Modified

$$\frac{d\delta_i}{dF} = 3 \times 10^{-5} \text{ in/kg}$$

Sp. No.	Crosshead speed cm/min	$\frac{dM}{dT}$ $\frac{\text{kg-cm}}{\text{min}}$	$\frac{d\delta_i}{dT}$ $\frac{\text{in/min}}{\times 10^5}$	$\frac{d\delta_s}{dT}$ $\frac{\text{in/min}}{\times 10^5}$	Estimated $\frac{d\delta}{dT}$ $\frac{\text{in/min}}{\times 10^5}$	Exp + l $\frac{d\delta}{dT}$ $\frac{\text{in/min}}{\times 10^5}$
1	0.02	24.8	19.5	33.7	53.2	50.3
2	0.002	2.51	1.97	3.81	5.78	5.45
3	0.0002	0.251	0.197	0.349	0.546	0.502
4	0.00002	0.024	0.018	0.032	0.05	0.046
5	0.005	6.24	4.91	8.41	13.3	12.46
6	0.0005	0.629	0.495	0.841	1.33	1.20
7	0.0002	0.251	0.197	0.359	0.556	0.527
8	0.00002	0.024	0.018	0.052	0.07	0.066
9	0.0005	0.629	0.495	0.783	1.27	1.01

Material: SiC (ceradyne)

Test: Modified

Specimen: CMB

Sp. No.	Crosshead speed cm/min	$\frac{dM}{dt}$ kg-cm	$\frac{d\delta_i}{dT}$ $\times 10^5$ in/min	$\frac{d\delta_s}{dT}$ in/min $\times 10^5$	Estimated $\frac{d\delta}{dT}$ in/min $\times 10^5$	Exptl $\frac{d\delta}{dT}$ in/min $\times 10^5$
1	0.002	2.54	2.0	2.62	4.62	4.23
2	0.0002	0.255	0.2	0.259	0.459	0.43
3	0.00002	0.0259	0.02	0.026	0.046	0.0415

Material: SiC (REFL)

Test: Modified

Specimen: CMB

Sp. No.	Crosshead speed cm/min	$\frac{dM}{dT}$ kg-cm min	$\frac{d\delta_i}{dT}$ in/min $\times 10^5$	$\frac{d\delta_s}{dT}$ in/min $\times 10^5$	$\frac{d\delta}{dT}$ Estimated in/min $\times 10^5$	Exptl. $\frac{d\delta}{dT}$ in/min $\times 10^5$
1	0.00002	0.025	0.019	0.036	0.055	0.049
2	0.0002	0.256	0.201	0.338	0.539	0.51
3	0.0002	0.259	0.203	0.487	0.60	0.656
4	0.002	2.61	2.05	3.93	5.98	5.21
5	0.00002	0.025	0.052	0.019	0.033	0.047

Fig. 1 Testing the performance of the jig with CMB tool steel specimen.

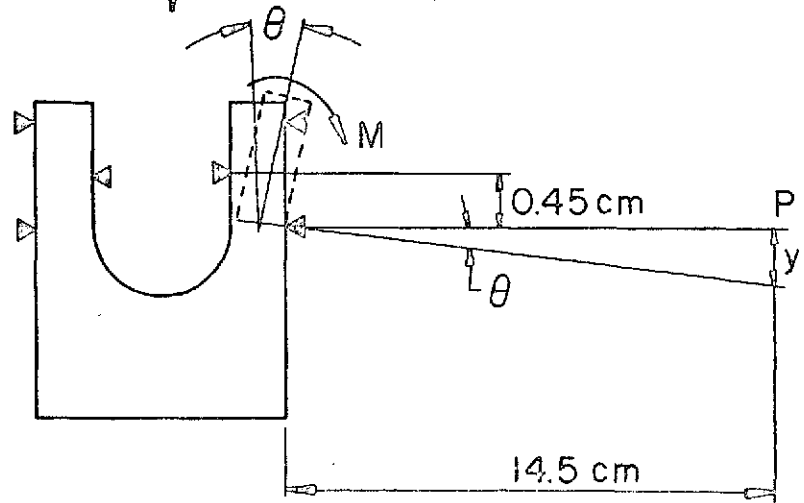
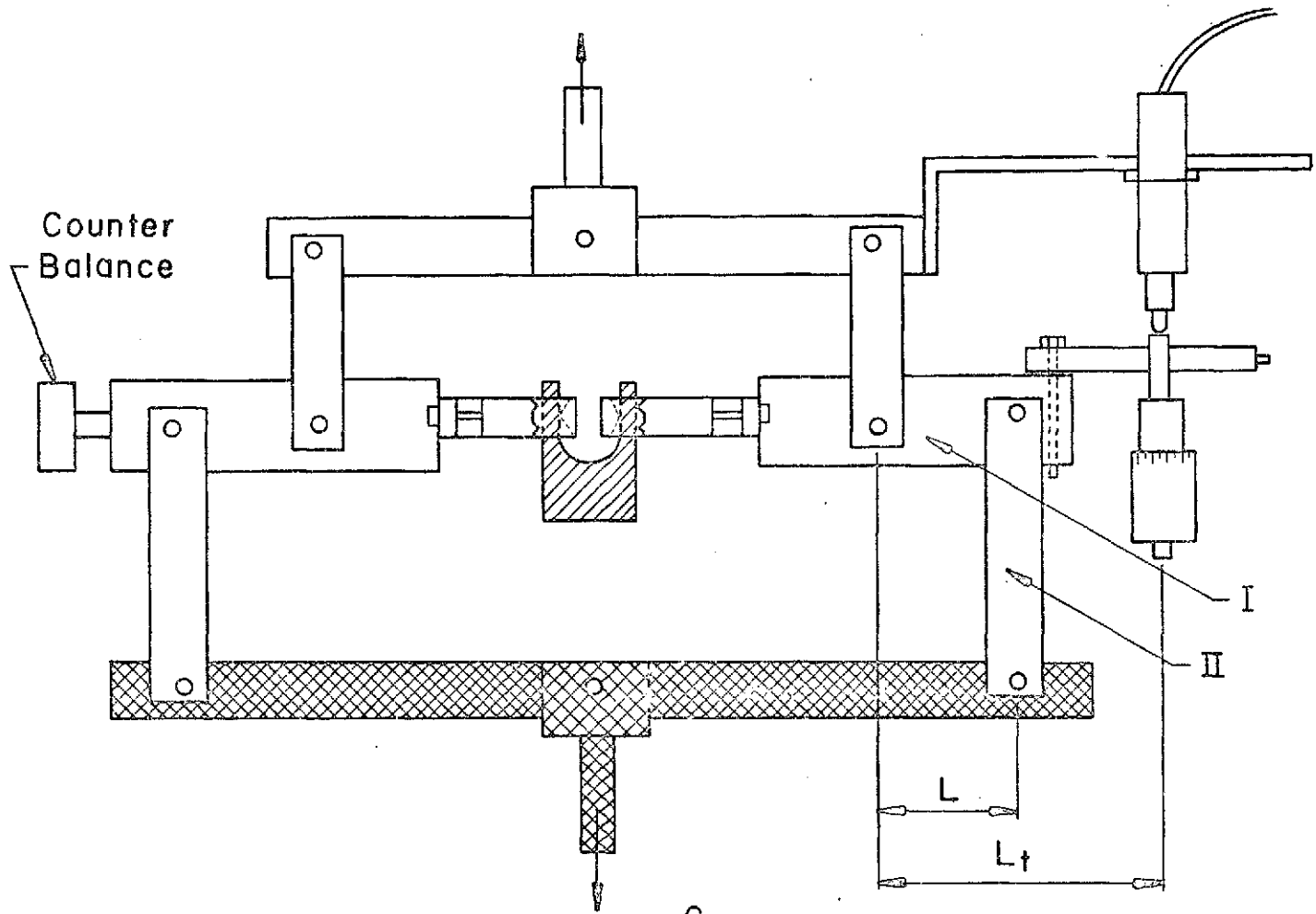


Fig. 2 Schematic diagram of the elastic deformation of the specimen arms.

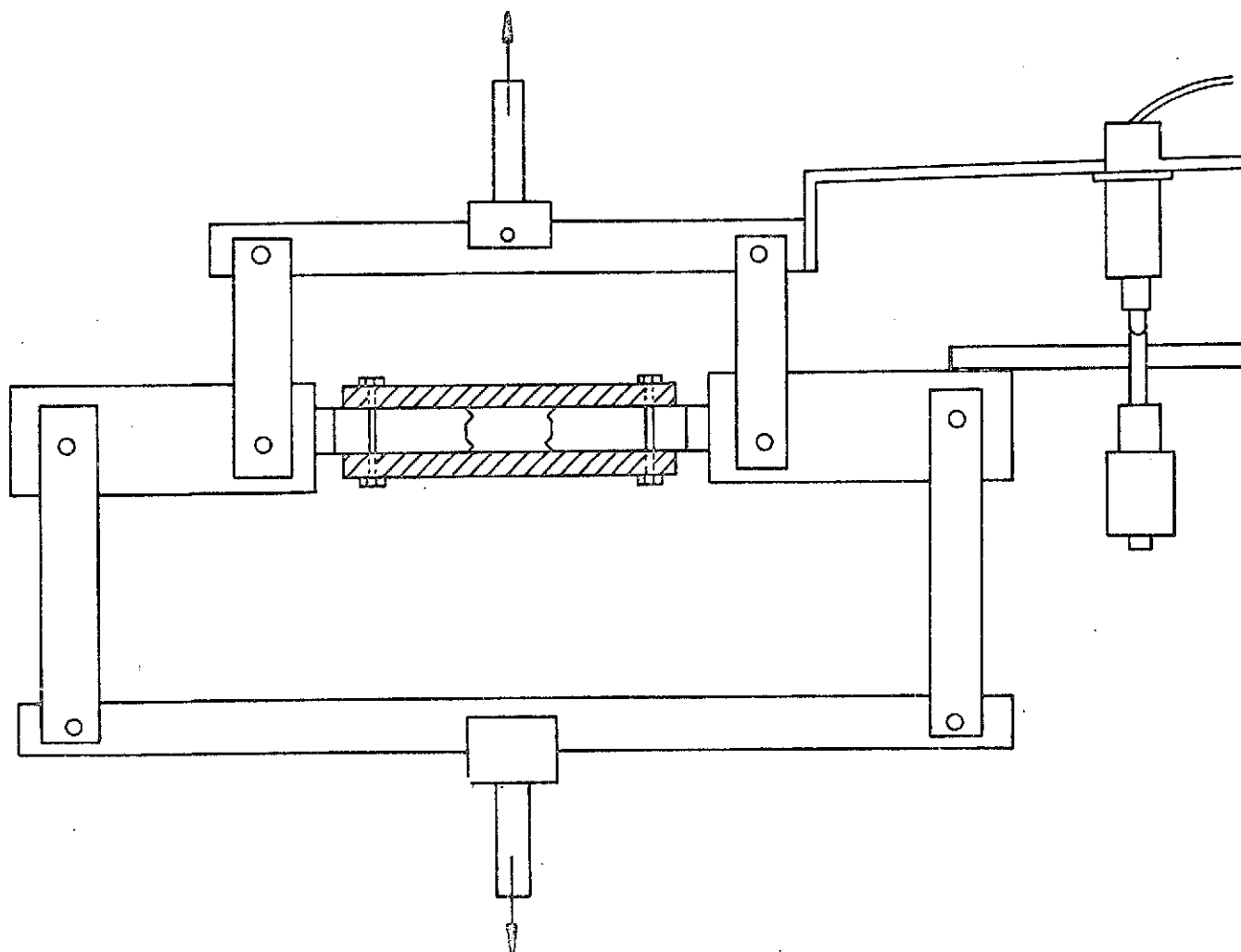


Fig. 3. Testing the performance of the jig with steel plates fastened to its arms.

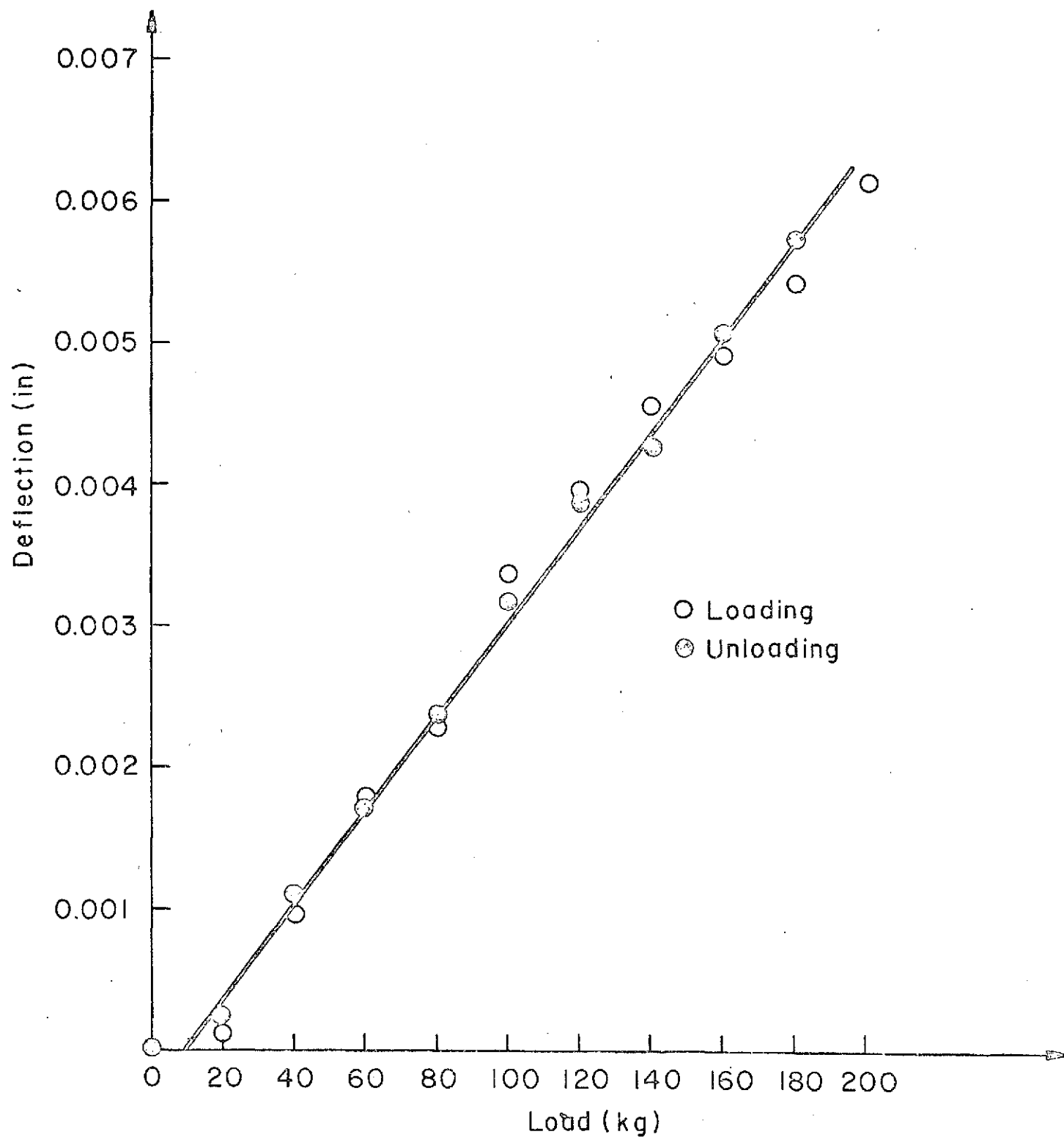


Fig. 4. Plot of load vs. deflection: Jig testing with steel plates fastened to its arms.

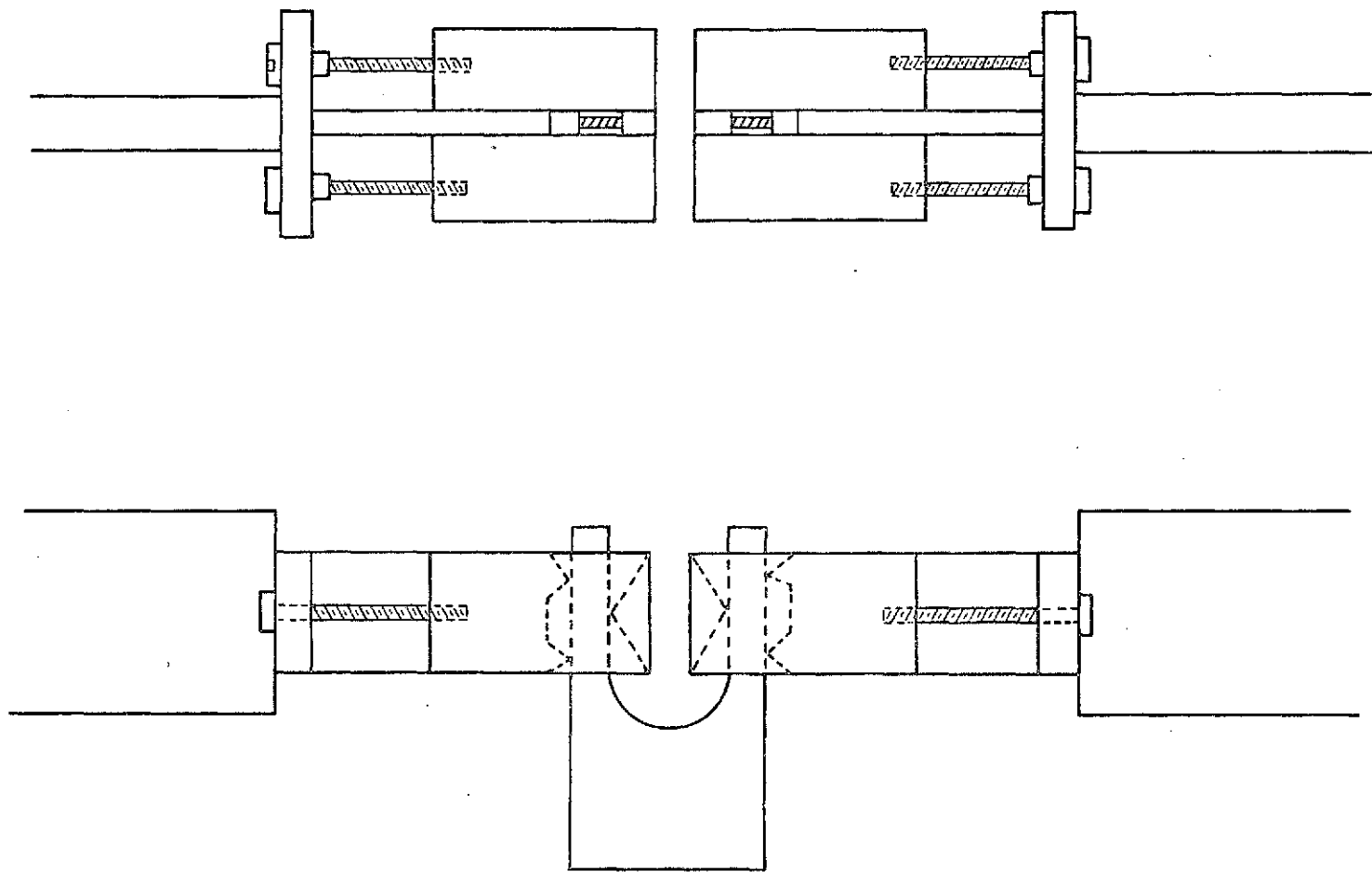


Fig. 5. The three-line grip with CMB specimen.

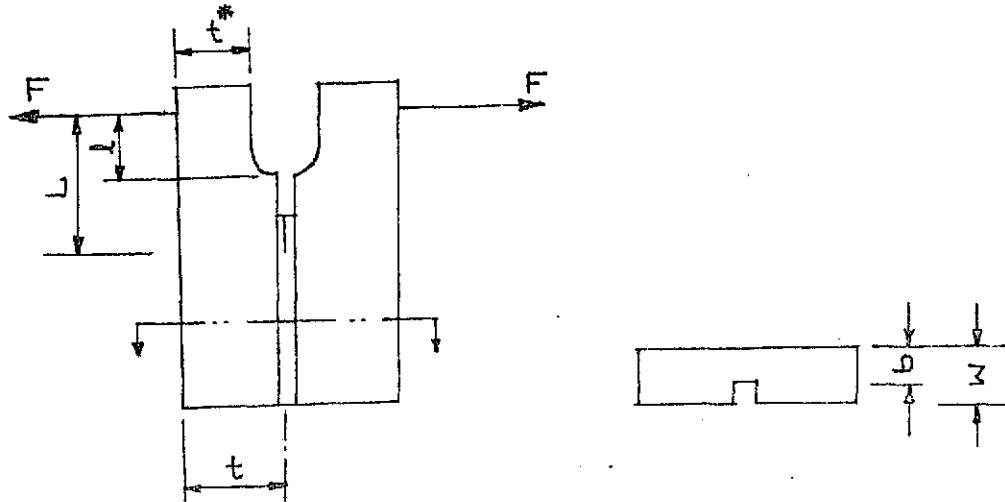


Fig. 6a-Double Cantilever Beam (modified arm)

eqn. I

$$G = \frac{12 F^2 L^2}{E W b t^3} \left\{ 1 + \left(\frac{\ell}{L} \right)^2 \left[\left(\frac{t}{t^*} \right)^3 - 1 \right] + 1.32 \frac{t}{L} \left(1 + \left(\frac{\ell}{L} \right) \left[\left(\frac{t}{t^*} \right)^2 - 1 \right] \right) \right\} \\ + 0.542 \left(\frac{t}{L} \right)^2 \left(1 + \left(\frac{\ell}{L} \right)^2 \left[\left(\frac{t}{t^*} \right)^2 - 1 \right] \right)$$

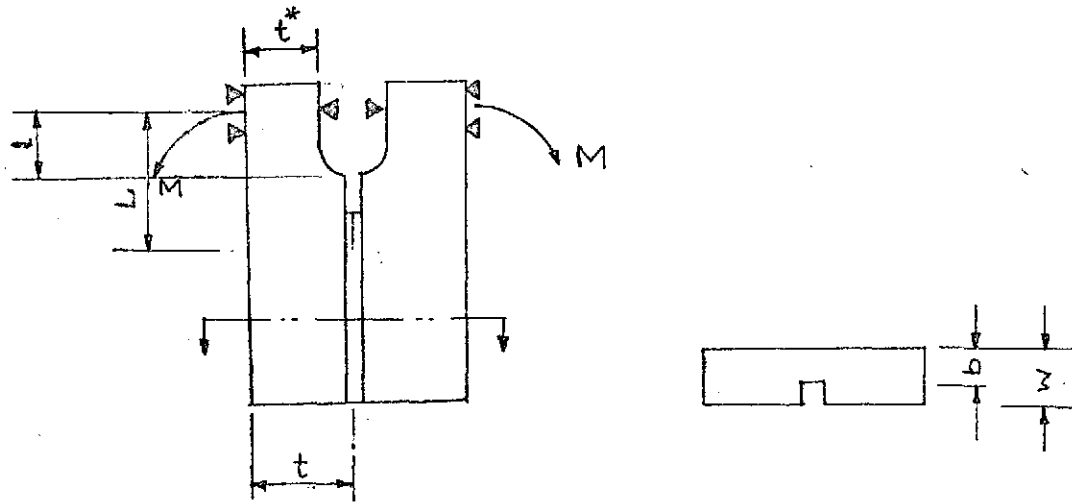


Fig. 6b - Constant Moment Beam (modified arm)

eqn. II

$$G = \frac{12 M^2}{E W b t^3} \left\{ 1 + \left(\frac{\ell}{L} \right)^2 \left[\left(\frac{t}{t^*} \right)^3 - 1 \right] \right\}$$

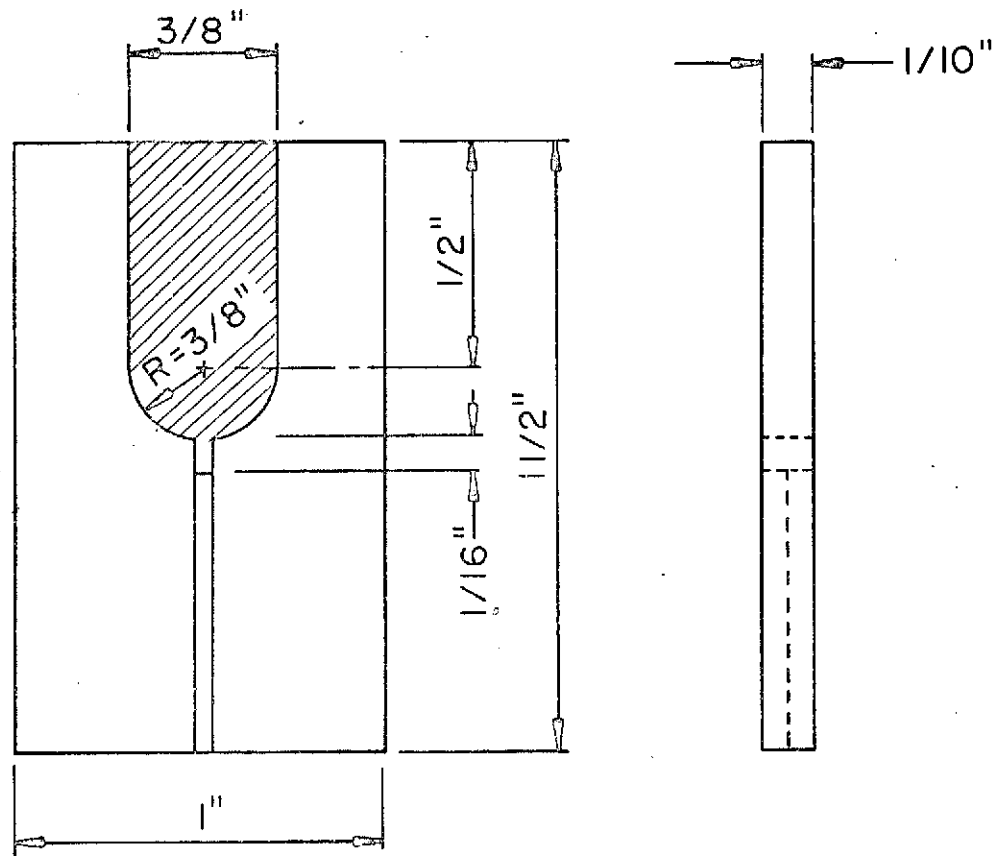


Fig. 7. Constant Moment Beam Specimen.

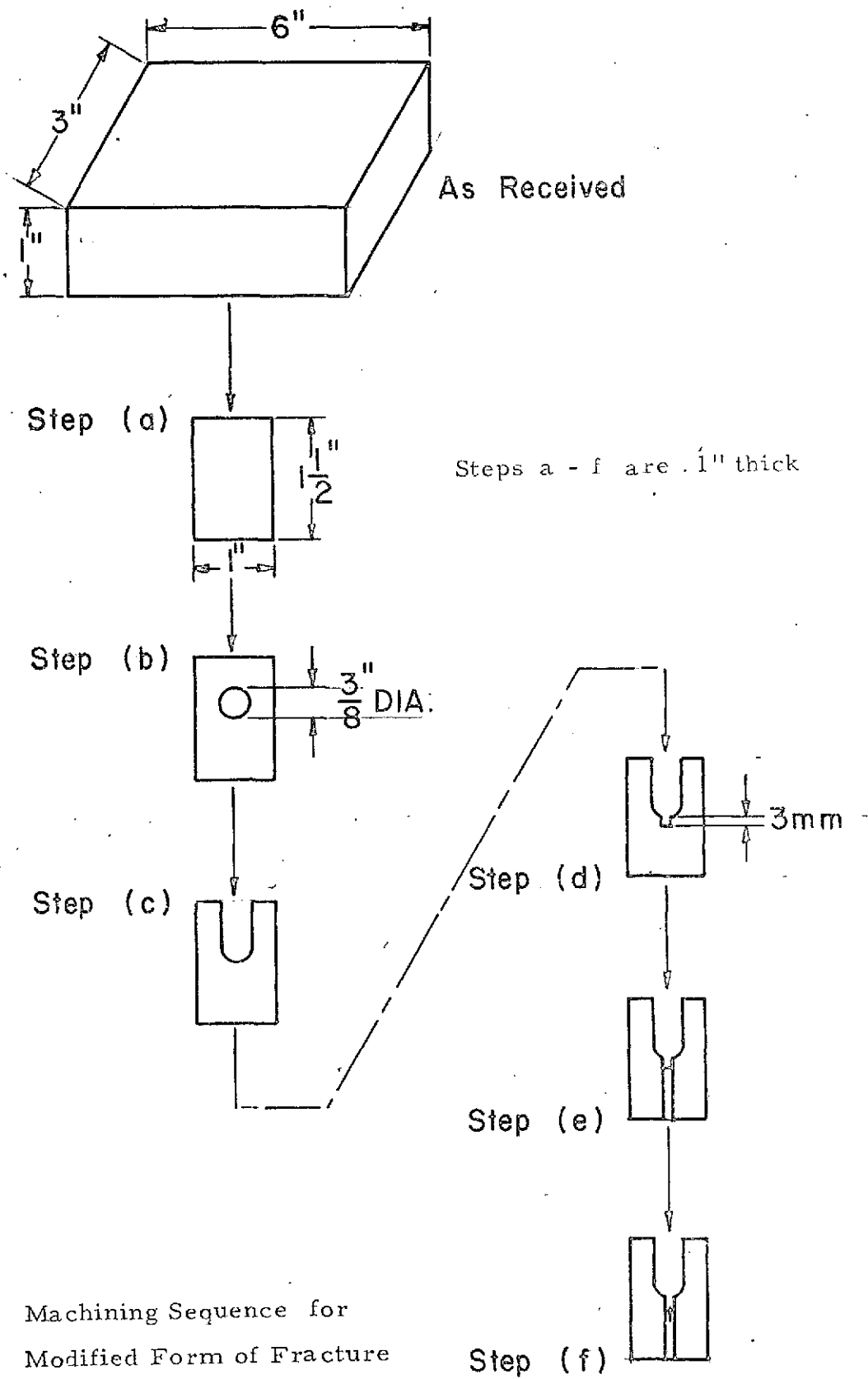


Fig. 8. Machining Sequence for Modified Form of Fracture Specimen

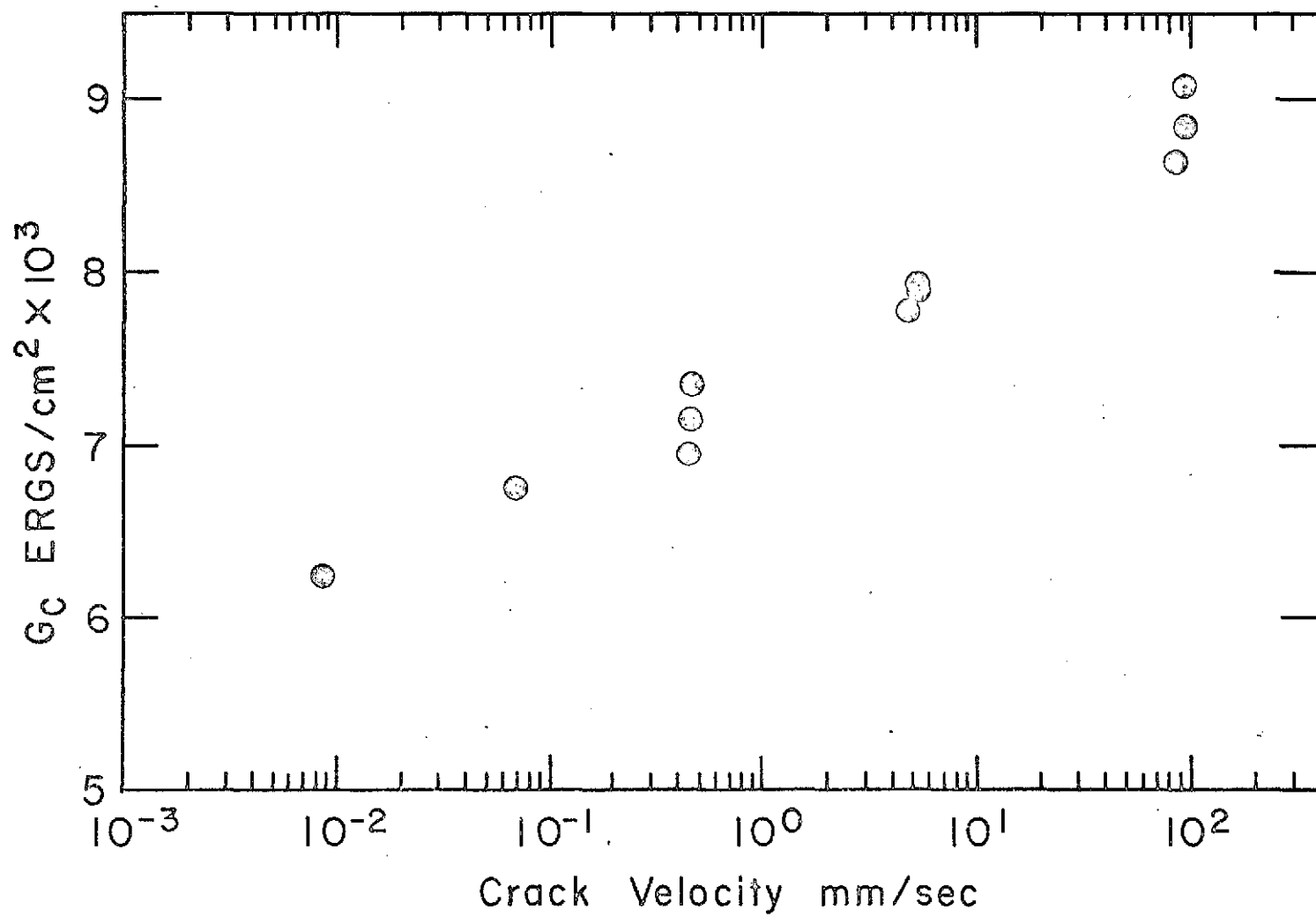


Fig. 9 G_c for slow crack growth in glass microscope slides in room air using constant moment test.

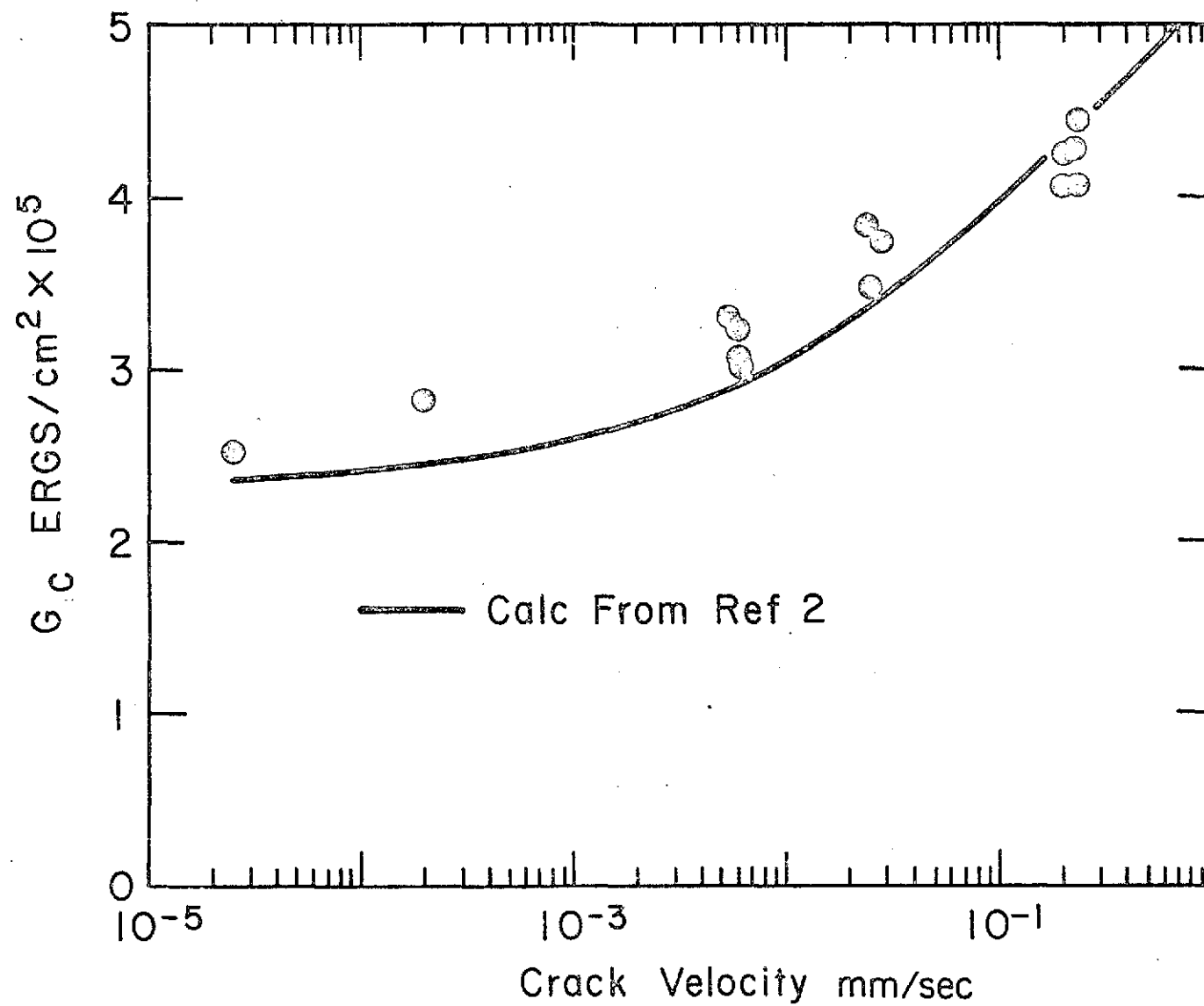
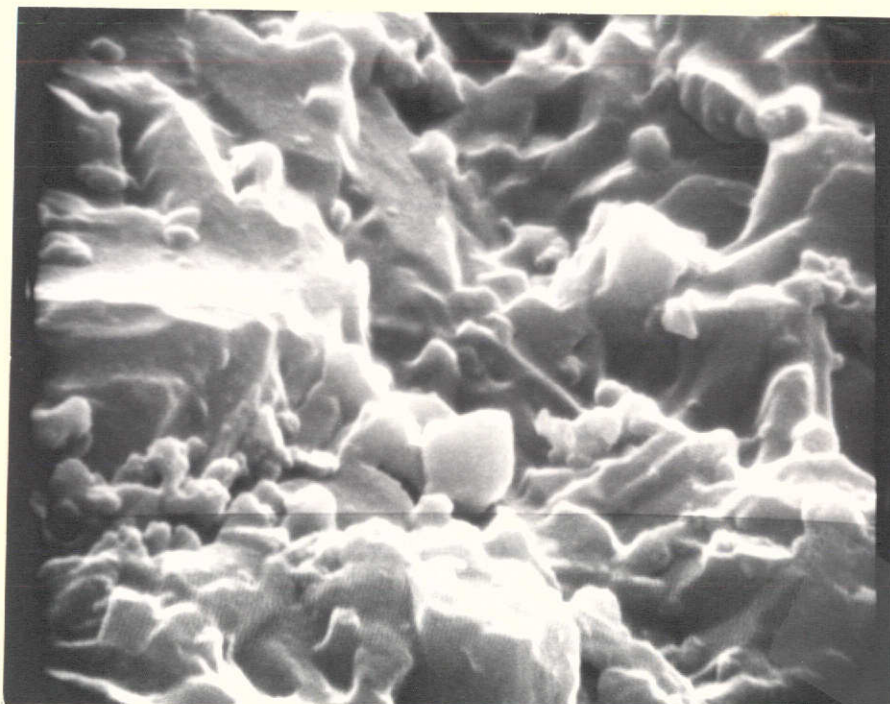


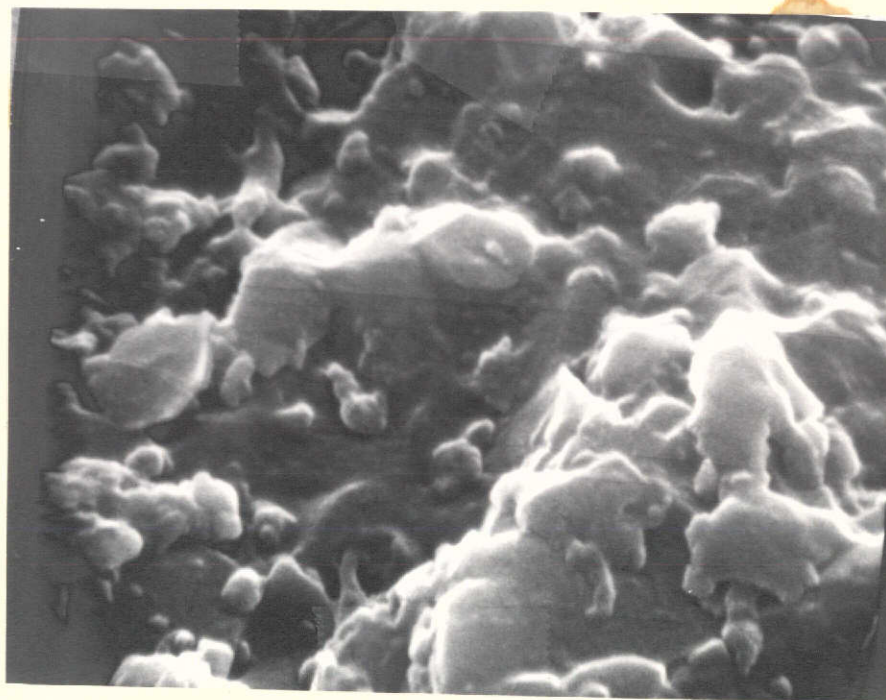
Fig. 10 G_c for slow crack growth in plexiglass in room air using constant moment test.



NOT REPRODUCIBLE

← Direction of crack propagation

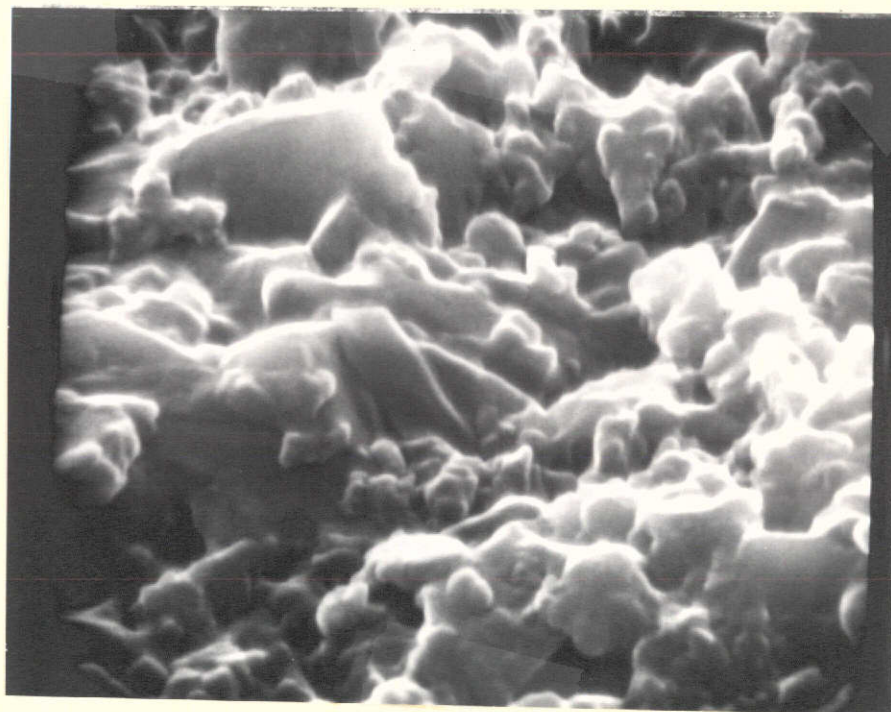
Fig. 11. H. P. Si_3N_4 (HS-130 Norton) fractured by CMB test.
Crosshead speed 0.00002 cm/min. Magnification
20,000 X.



NOT REPRODUCIBLE

← Direction of crack propagation

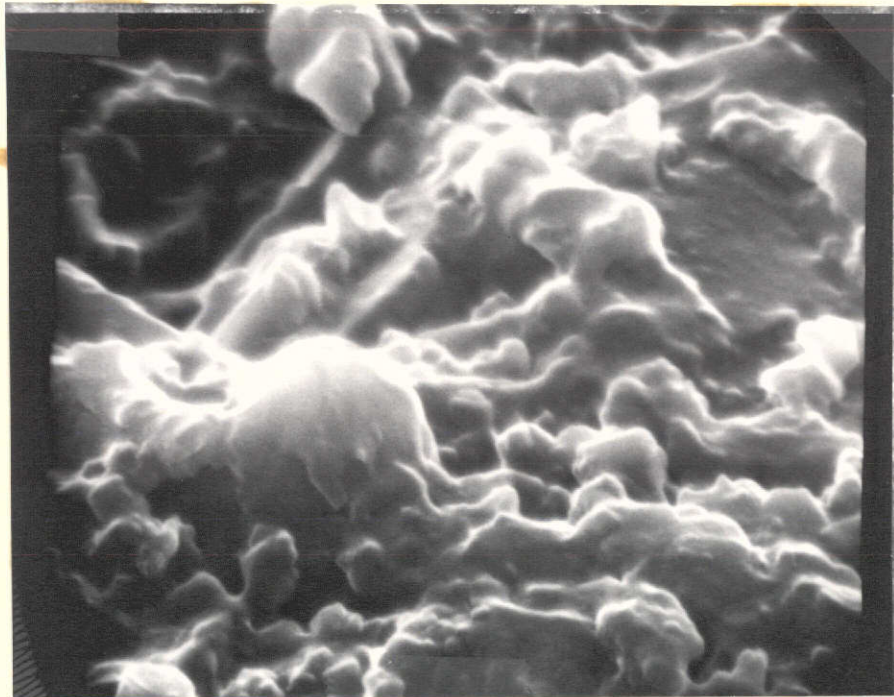
Fig. 12. H. P. Si_3N_4 (HS-130 Norton) fractured by CMB test. Cross-head speed 0.0002 microcrack portion. Magnification 21000 X.



NOT REPRODUCIBLE

← Direction of crack propagation

Fig. 13. H. P. Si_3N_4 (H.S. -130 Norton) fractured by CMB test. Crosshead speed 0.0002 cm/min. Fast crack propagation portion. Magnification 22000X.



NOT REPRODUCIBLE



Direction of crack propagation

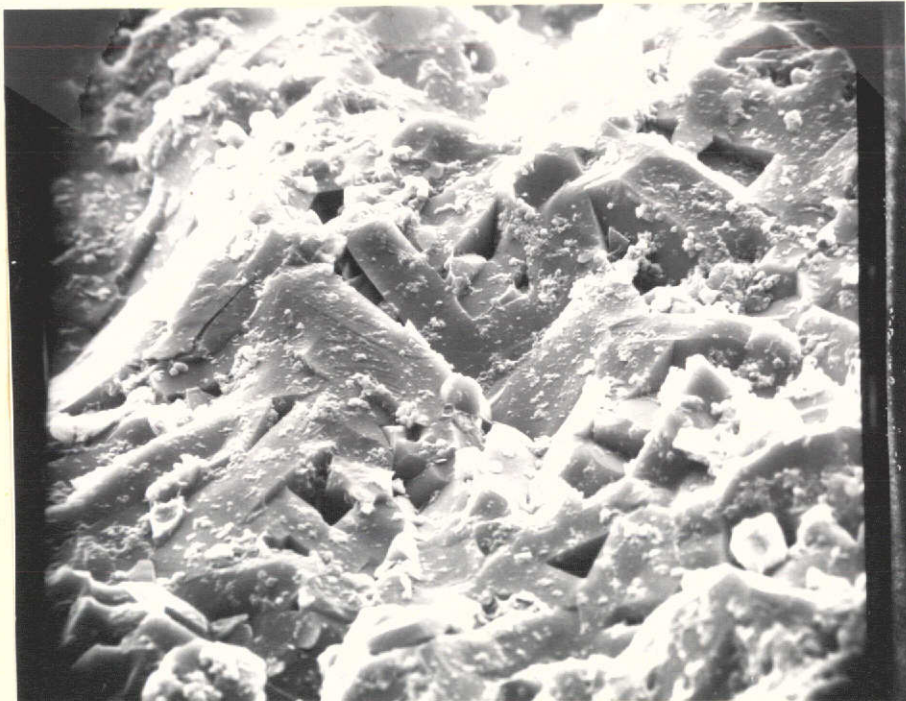
Fig. 14. H. P. Si_3N_4 (HS-130 Norton) fractured by DCB.
Magnification 22000X.



NOT REPRODUCIBLE

→ Direction of crack propagation

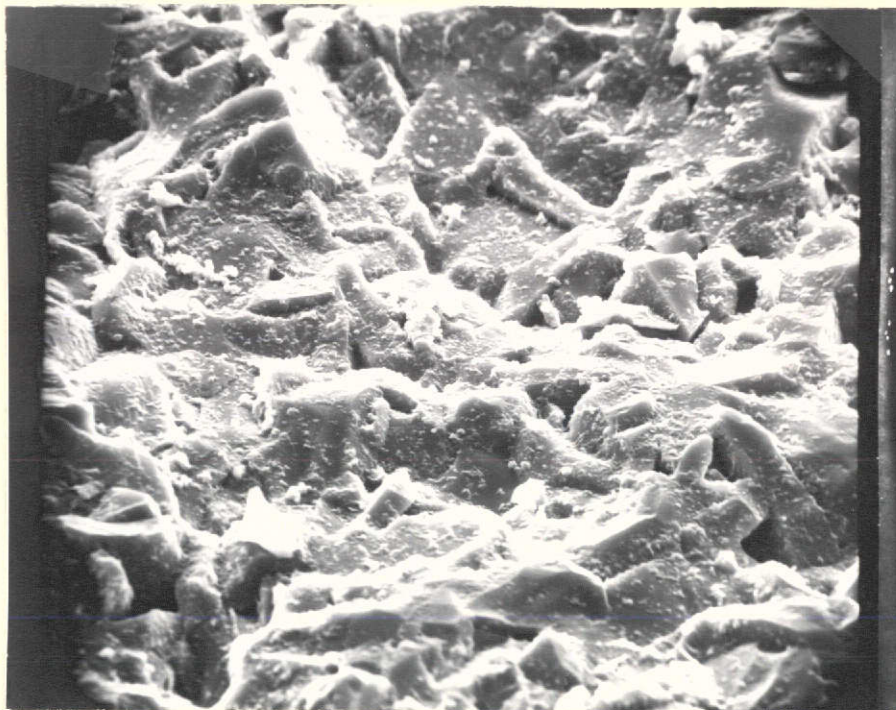
Fig. 15. SiC (Ceradyne) fractured by CMB test. Crosshead speed 0.0002 cm/min. Magnification 1100X.



NOT REPRODUCIBLE

→ Direction of crack propagation

Fig. 16. SiC (Ceradyne) fractured by CMB test. Crosshead speed cm/min. Magnification 1150X.



NOT REPRODUCIBLE



Direction of crack propagation

Fig. 17. SiC (Ceradyne) fractured by CMB test. Crosshead speed 0.00002 cm/min. Magnification 1000X.



NOT REPRODUCIBLE



Direction of crack propagation

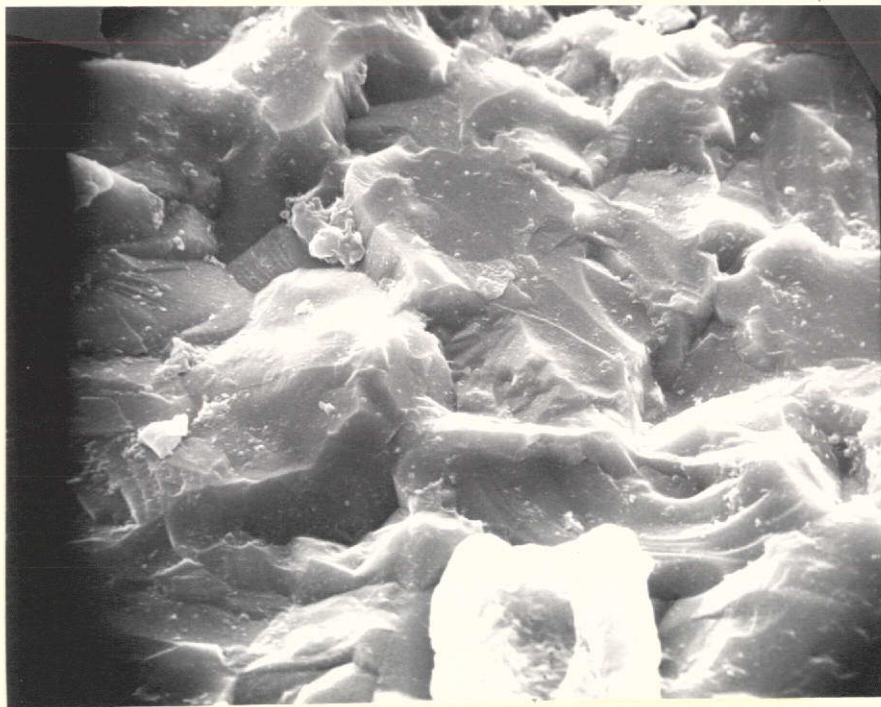
Fig. 18 SiC (REFEL) fractured by CMB test. Crosshead speed 0.0002 cm/min. Magnification 1900X.



NOT REPRODUCIBLE

← Direction of crack propagation

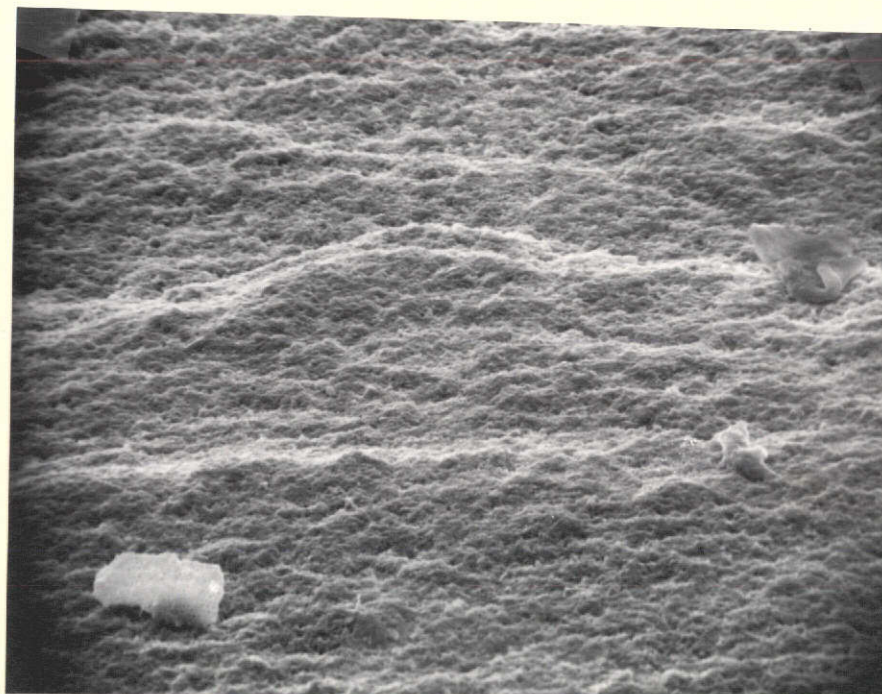
Fig. 19. SiC (REFEL) fractured by CMB test. Crosshead speed 0.002 cm/min. Magnification 2000X.



NOT REPRODUCIBLE

← Direction of crack propagation

Fig. 20. SiC (REFEL) fractured by CMB test. Crosshead speed
0.00002 cm/min. Magnification 2000X.



NOT REPRODUCIBLE



Direction of crack propagation

Fig. 21. H. P. Si_3N_4 (HS-130) fractured by CMB test. Crosshead speed 0.00002. Magnification 550X.



NOT REPRODUCIBLE

← Direction of crack propagation

Fig. 22. Same specimen as Fig. 21 but not exhibiting secondary phase particles and fracture lines.